Ultranarrow bandpass hybrid filter with wide rejection band

Julien Lumeau, Michel Cathelinaud, Jean Bittebierre, and Michel Lequime

The theoretical study and the experimental realization of an ultranarrow bandpass filter, joining a fiber Bragg grating and a dielectric mirror directly deposited at the extremity of the fiber tip, is presented. The features of such a filter are in very good accordance with the results of theoretical simulations. © 2006 Optical Society of America

OCIS codes: 050.2230, 050.7330, 310.1620, 310.6860.

1. Introduction

Ultranarrow bandpass filters (i.e., filters with spectral bandwidth less than 0.1 nm) are often used in demanding applications like astronomical observation or Raman scattering studies. They can be achieved with the help of two main manufacturing techniques: the first one uses all dielectric Fabry–Perot stacks with a thin spacer (few micrometers) and two high reflectance (typically 99.9%) dielectric mirrors (DMs), including a large number of layers (more than 100). The second one is based on a solid-spaced etalon (SSE),[1–3] i.e., a quite thick fused-silica wafer (typically 100 μm or more) acting as the spacer of a Fabry–Perot cavity and the both sides of which are coated with standard performance DMs (reflectivity of approximately 96%). This last solution is very attractive in term of number of layers, but its free-spectral range (FSR) is small (typically 8 nm for a 100-μm etalon), which induces the appearance of numerous unwanted transmission peaks in the useful spectral range (for instance the C-Band in the case of telecommunications applications). To suppress these parasitic peaks, a first solution is to use an autofiltering cascaded SSE[4,5] (i.e., for instance, two coherently coupled SSE with different FSR), but with this use it is difficult to obtain a very large rejection band (more than 100 nm). Another method consists of replacing one of the broadband mirrors used in a SSE with a spectrally selective structure whose reflectivity is important only around the central wavelength of the filter. Such a behavior can be easily obtained by inscribing a Bragg grating structure in the thickness of the SSE. This association [volume Bragg grating (VBG) + DM], henceforth called a hybrid filter, was recently proposed in a guided configuration.[6] This paper is devoted first to the description of a phenomenological approach that permits a fast definition of the filter properties and second to the presentation of some experimental results from this guided configuration.

2. Theoretical Approach

A. Basic Structure Analysis

The typical structure of a hybrid filter is represented on the Fig. 1. In accordance with the definition given in the previous section, it includes two main items, i.e., a VBG or a FBG and a DM. We can see on this figure a third element, called matching layer (ML), defined by a thickness e and a refractive index n_L, but the purpose of this new item will be explained in Subsection 2.B, and we can assume for this first section that its thickness is equal to zero.

The refractive-index modulation associated to the VBG is defined by

$$n(z) = n_0 + \Delta n \sin\left(2\pi \frac{z}{\Lambda} + \phi\right), \tag{1}$$

where n_0 is the mean value of this refractive-index profile, Δn the modulation amplitude, ϕ the start phase (phase of the modulation at $z = 0$), and Λ the pitch of the sine modulation. The length of the mod-

The authors are with the Institut Fresnel - Unité Mixte de Recherche, Centre National de la Recherche Scientifique 6133, Université Paul Cézanne-EGIM-Université de Provence, Domaine Universitaire de Saint-Jérôme, 13397 Marseille, Cedex 20, France. J. Lumeau's e-mail address is jlumeau@creol.ucf.edu.

Received 2 March 2005; accepted 30 June 2005.
0003-6935/06/071328-05$15.00/0

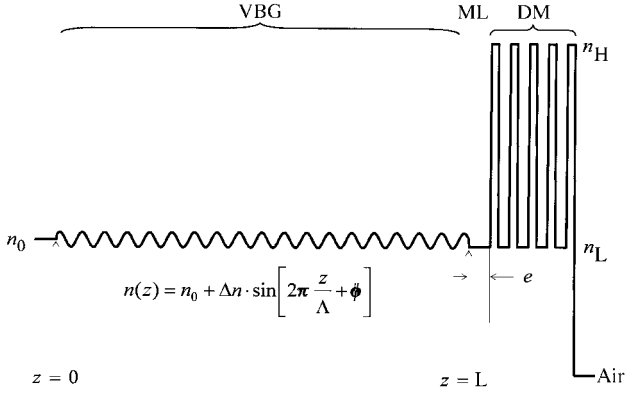

Fig. 1. Schematic representation of a hybrid filter, including a VBG, an ML, and a DM.

ulated zone is supposed equal to L. This structure is immerged into a transparent photosensitive substrate whose refractive index is again equal to n_0. The central wavelength of this Bragg mirror is therefore defined $\lambda_0 = 2n_0\Lambda$.

The DM is described by its spectral reflectivity $R_1(\lambda)$, which is directly connected to the number of the quarter-wave alternated layers used for its manufacturing, and by the choice of the low- and high-index materials (for instance, SiO_2 and Ta_2O_5).

Let us suppose now that the photosensitive substrate is semi-infinite (which is a quite good description of a guided configuration) or that the rear face of this substrate is coated with an antireflective coating (which can be easily achieved in the case of a VBG). To simulate theoretically the spectral transmittance of such a structure, we have performed first a decomposition of the modulated zone into a stack of thin homogeneous layers (with for each layer a refractive index equal to the mean value of the refractive-index profile into this layer), thus we have applied to this virtual stack a classical thin-films matrix formalism.[7,8] The performances of our hybrid filter seem a critical function of the phase quantity Φ associated to this specific structure and defined

$$\Phi = \left(\phi + 2\pi \frac{L}{\Lambda}\right) + \varphi_{DM}(\lambda_0), \tag{2}$$

where $\varphi_{DM}(\lambda_0)$ is the phase variation at the reflection on the DM for the central wavelength of the Bragg grating structure.

To achieve a filter with optimal spectral transmittance performances, as presented at the Fig. 2, this phase term shall be exactly equal to zero (modulo 2π). Figures 2(a) and 2(b) show in this case (resonance condition fulfilled) the features of a hybrid filter in a large spectral range (1200–1900 nm) and near the design wavelength (1547–1553 nm), respectively. This hybrid filter is described by the following set of parameters:

- Bragg grating structure—central wavelength, $\lambda_0 = 1550$ nm; length, $L = 1.6$ mm; mean refractive index, $n_0 = 1.46$; refractive-index modulation amplitude $\Delta n = 5.3 \times 10^{-4}$
- DM—number of layers, 7; high-index layer, Ta_2O_5 ($n_H = 2.12$); low-index layer, SiO_2 ($n_L = 1.44$)

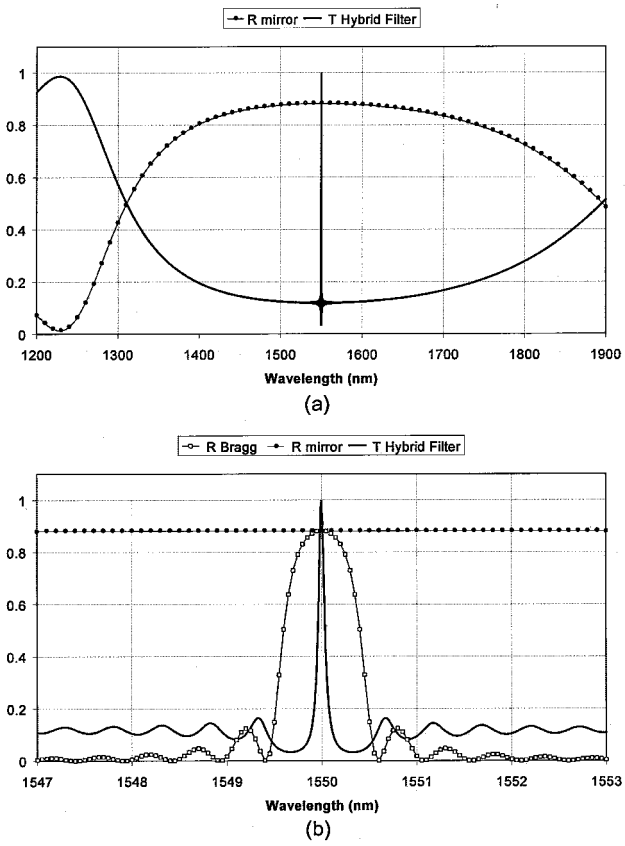

Fig. 2. Theoretical transmission of a hybrid filter (a) in a wide spectral range and (b) close to the central wavelength. The hybrid filter includes a VBG (central wavelength, 1550 nm; length, 1.6 mm; mean refractive index, 1.46; modulation amplitude, 5.3×10^{-4}; reflectivity, 88%) and a DM (number of layers 7, high-index layer Ta_2O_5, low-index layer SiO_2, reflectivity 88%).

In Fig. 2(a) we note, as expected, the presence of a single transmission peak in the whole spectral range but also the moderate value of the rejection level around the peak wavelength. This last feature is indeed completely defined by the reflectance properties of the DM and can be thus improved by simply increasing the number of alternated layers. Figure 2(b) shows the shape of the Bragg grating reflectance and the spectral profile of the hybrid filter close to the design wavelength. The peak VBG reflectance $R_2(\lambda_0)$ is directly connected to the product $L\ \Delta n$ and can be estimated with the theoretical relation[9]

$$R_2(\lambda_0) = \tanh^2\left(\frac{\pi L \Delta n}{\lambda_0}\right). \tag{3}$$

This value shall be matched to the reflectance of the DM at the same wavelength to maximize the filter transmission. Indeed, this quantity is defined by the classical Fabry–Perot transmittance relation

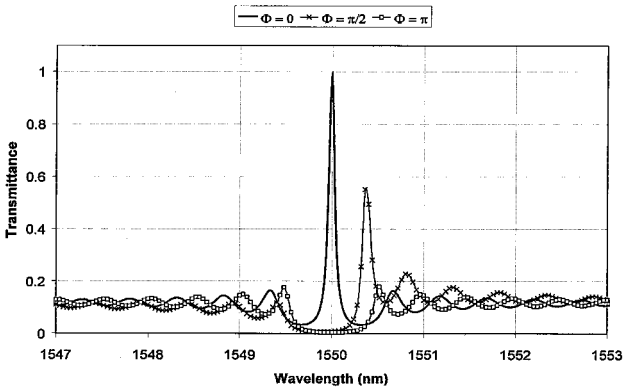

Fig. 3. Influence of the phase term on the spectral profile. The main features of the hybrid filter are identical to the ones given in the Fig. 2.

$$T_{\max} = \frac{(1 - R_1)(1 - R_2)}{(1 - \sqrt{R_1 R_2})^2} \tag{4}$$

and is equal to 100% only for identical VBG and DM reflectance.

If the resonance condition is not fulfilled, i.e., if the phase quantity Φ is not equal to zero, the performances of the hybrid filter can be deeply modified, as represented at the Fig. 3, in two specific cases corresponding to $\pi/2$ and π phase values. In this last case, the structure is antiresonant, which leads to a complete disappearance of the transmission peak. In the intermediate $\pi/2$ case, we note a shift of the peak wavelength in the Bragg envelope associated to a decreasing of its maximal transmittance.

The last important parameter connected with the design of such a filter is the value of the full bandwidth at half maximum (FWHM) $\delta\lambda$ of the transmission peak in a resonant configuration. This quantity can be estimated, again, by use of a classical Fabry–Perot relation, i.e.,

$$\delta\lambda = \frac{{\lambda_0}^2}{2n_0 t} \frac{1 - \sqrt{R_1 R_2}}{\pi (R_1 R_2)^{1/4}}, \tag{5}$$

where t is a composite parameter that can be described as the distance between the DM and a virtual mirror whose reflectivity is equal to the VBG one and that is located inside the VBG, at a distance linearly increasing with the VBG length for a given refractive-index modulation. With the numerical data previously used, this virtual distance is approximately 400 μm, which leads to a FWHM bandwidth close to 85 pm.

B. Matching Layer Structure

With the help of the theoretical approach that we detailed in the previous section and which combines numerical simulations and phenomenological descriptions, we designed a hybrid filter in accordance with a given set of specifications, like maximal transmittance, peak wavelength, bandwidth, and so on. But reaching the optimal level of performances required strictly satisfying the resonance condition (phase quantity equal to zero modulo 2π). The phase term associated to the DM being entirely defined by the stack structure means that it is required to control with a high accuracy the end phase of the modulation φ_f, defined

$$\varphi_f = \left(\phi + 2\pi \frac{L}{\Lambda}\right), \tag{6}$$

or, in other words, to control the fractional number of periods of the grating, which is obviously very difficult.

It is for this reason we have introduced a new item called ML in the global description of our hybrid filter (see Fig. 1). This extra layer, whose use is mandatory to envisage in a practical way the manufacturing of a such structure, is characterized by an optical thickness $n_L e$ (we assume here that this ML has the same refractive index as the low-index layer used in the mirror stack, which corresponds to the actual configuration). In this case, the resonance condition becomes

$$\Phi = \left(\phi + 2\pi \frac{L}{\Lambda}\right) + 2\pi \frac{2n_L e}{\lambda_0} + \varphi_{\mathrm{DM}}(\lambda_0) = 0(2\pi), \tag{7}$$

which allows us to adjust the value of the overall phase term Φ to fulfill the resonance condition by simply controlling the mechanical thickness e of the matching layer.

3. Experimental Demonstration

To demonstrate in a simple way the potential performances of this kind of filter, we decided to use a guided configuration and supplied in accordance to the Advanced Optics Solutions GmbH company a FBG precisely located at the extremity of the fiber tip (the fiber is 0° cut in a plane corresponding to the last index oscillations of the grating). The main features of this grating (amplitude of the refractive-index modulation, length, and central wavelength) are quite similar to those used in the simulations presented in the previous sections.

We first performed a preliminary verification of our approach by using a metallic mirror (silvered mirror) placed in front of this FBG. This measurement scheme imposes use of reflectance data instead of transmittance ones. The adjustment of the ML was realized by changing the thickness of the air gap between the end of the FBG and the mirror. To precisely control the modifications of this distance, we fixed the mirror on a piezoelectric translation stage. The natural central wavelength of the FBG is equal to approximately 1549.6 nm. In Fig. 4, we see the evolution of the inverse reflectance peak (wavelength and value) for different positions (D_i) of the silver mirror, the mean distance between the mirror and the fiber extremity being approximately 100 μm. With such short distances, the reflection losses due to

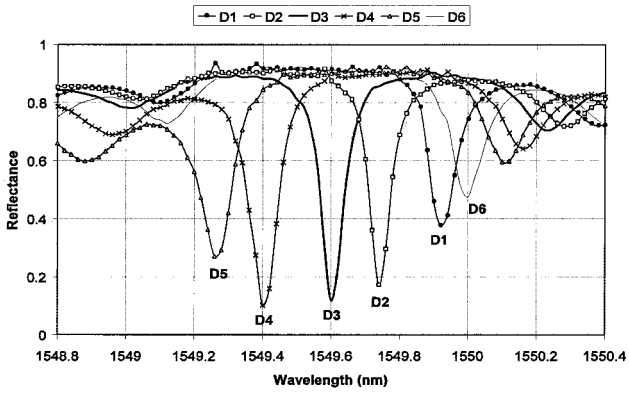

Fig. 4. Evolution of the spectral response of the hybrid filter with the position of the metallic mirror experimentally used instead of the DM. The various positions of the mirror correspond to different air gap thicknesses and then to different values of the phase term (D3 is close to the resonance, whereas D5 or D6 are close to the antiresonance).

the imperfect recoupling of the Gaussian beam into the fiber after reflection on the silvered mirror leads to an effective reflectance value of approximately 60% for the DM. The reflectance of the FBG being equal to approximately 83% means that the transmittance peaks will not be equal to 100%: it is exactly what is observed on the spectral reflectance data, recorded with the help of an EXFO FLS 2600 Tunable Laser Source (tuning range 1520–2570 nm, spectral resolution 10 pm). We see also in Fig. 4, how the transmittance peak is moving in the FBG spectral lobe, which confirms, if needed, the possibility of correcting the final phase of the hybrid filter with the help of an interstitial layer deposited at the surface of the fiber tip.

To achieve a more complete validation of such a filter, we deposited quarter-wave-alternated DM at the end of the FBG by classical electron-beam deposition. The thickness monitoring of each layer was realized with an *in situ* measurement of the reflectance of the assembly, with the help of the tunable laser source presented before, and connected to the FBG through a 3-dB coupler and a fiber-tight throughfeed. The control was realized at a single wavelength, and we also performed a complete spectral measurement of the filter reflectance properties after each important layer, i.e., after the first layer (adaptation layer) and at the end of each mirror (M_{2i+1}, with i integer). The deposition sequence was the following: we started by depositing a YF_3 ML to correct the end phase of the FBG and continued with an M9 (ZnS/YF_3) mirror, to reach a quite high rejection ratio (>90%). After deposition, we carried out transmittance measurement in air of this hybrid filter around the resonance wavelength (1547–1553 nm) and in a wide spectral range (1200–1700 nm). The comparison of these experimental results with the theoretical predictions is presented in Fig. 5.

We see on these graphs that there is a very good agreement between theoretical and experimental

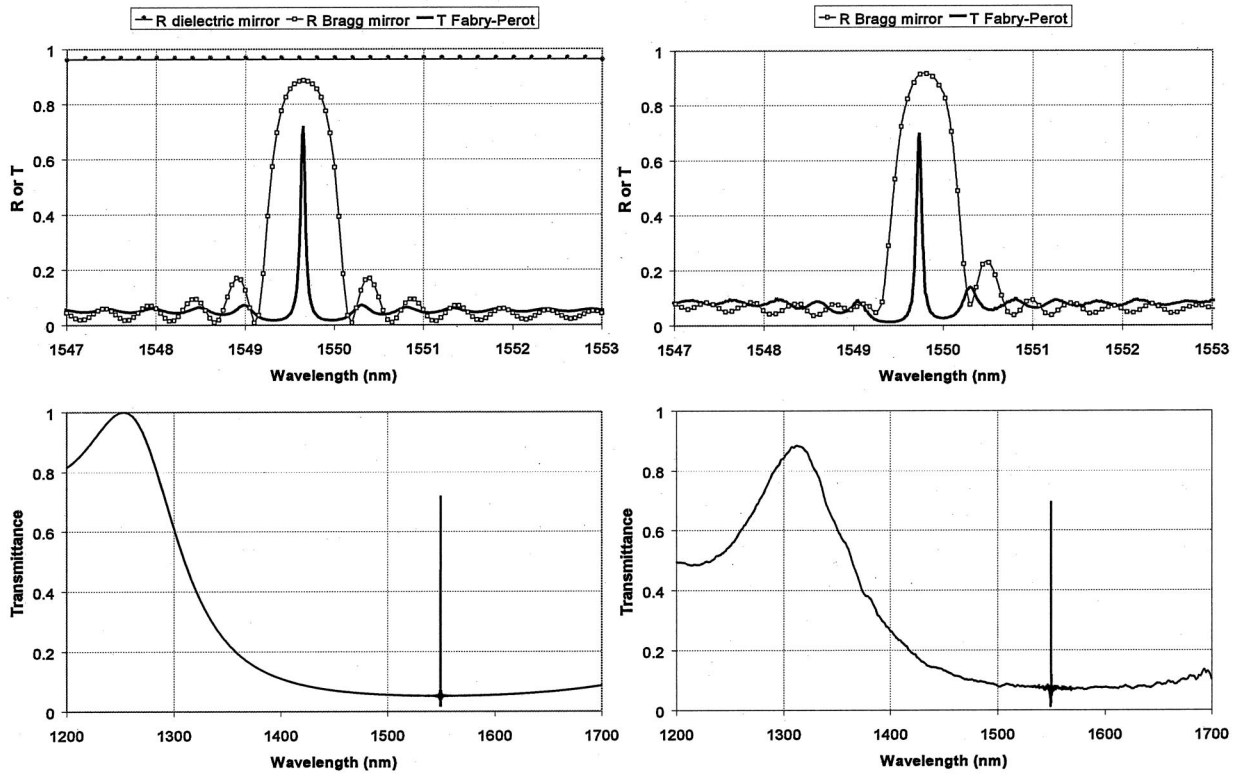

Fig. 5. Comparison between theoretical predictions (left column) and experimental results (right column) for a hybrid filter manufactured by depositing an M9 DM (ZnS/YF_3) at the extremity of a FBG Grating through a YF3 ML.

data and that there is a single narrowband resonance peak centered on 1549.6 nm and with a bandwidth of approximately 80 pm. However, we also notice that the maximal transmittance is not equal to 100% owing to the reflectance of the M9 DM being slightly higher that the Bragg mirror's one. The use of an M7 configuration did not allow us to overcome this problem, because of the rapid variation of the DM reflectance with the number of layers (with an M7 stack, the reflectance was this time slightly too low, and the rejection level was again reduced). We shall also stress the presence of some sidelobes around the central peak, probably the result of the FBG not being apodised.

4. Conclusion and Perspectives

We have presented a complete theoretical study and the first experimental results from a hybrid filter joining a FBG and a reflective dielectric stack. This filter is characterized by an ultranarrow bandwidth and wideband rejection properties, and we have shown that theoretical and experimental results are in very good accordance. The use of a ML inserted between the reflective stack and the surface of the VBG is a key point to allow the practical realization of such a structure. This ML can be manufactured at the beginning of the coating step before deposition of the DM.

To improve the rejection level in the stop band, we can either increase the number of layers used in the dielectric stack (but in this case, the reflectance of the DM part will become rapidly greater than the VBG one, which leads to a decrease of the maximal transmittance of the filter), or increase simultaneously the efficiency of the two reflective structures, but the virtual thickness rapidly increases, inducing a correlated decrease of the filter bandwidth.

To increase this rejection level and obtain at the same time a more squared shape for the filter profile in its transmission window, another possible solution is to use a tandem configuration joining two identical hybrid filters in a symmetrical arrangement (i.e., by associating the two structures by their DMs through a coupling layer). The theoretical simulations of such a symmetrical tandem arrangement are very promising, and its practical implementation in a guided configuration remains feasible.

Nevertheless, the use of a free-space configuration joining two photosensitive SSEs provides in this case a more attractive solution, especially for the final assembly of the two identical filters by optical contacting. We have started some practical and promising studies on this topic in close cooperation with the Photoinduced Processing Laboratory of Leonid Glebov (CREOL/UCF), which has manufactured, in this goal, dedicated VBGs in thin Photo-Thermo-Refractive (PTR) glass plates.[10]

References

1. J. A. Dobrowolski, "Mica interference filters with transmission bands of very narrow half-widths," J. Opt. Soc. Am. **49,** 794–806 (1959).
2. R. R. Austin, "The use of solid etalon devices as narrowband interference filters," Opt. Eng. **11,** 68–69 (1972).
3. A. E. Roche and A. M. Title, "Tilt tunable ultra narrow-band filters for high resolution photometry," Appl. Opt. **14,** 765–770 (1975).
4. J. Floriot, F. Lemarchand, and M. Lequime, "Double coherent solid-spaced filters for very narrow-bandpass filtering applications," Opt. Commun. **222,** 101–106 (2003).
5. J. Floriot, F. Lemarchand, and M. Lequime, "Cascaded solid-spaced filters for DWDM applications," in *Advances in Optical Thin-Films*, C. Amra, N. Kaiser, and H. A. Macleod, eds., Proc. SPIE **5250,** 384–392 (2003).
6. J. Bittebierre and B. Lazarides, "Narrow-bandpass filters with broad rejection band for single-mode waveguides," Appl. Opt. **40,** 11–19 (2001).
7. M. G. Moharam and T. K. Gaylord, "Chain matrix analysis of arbitrary-thickness dielectric reflection gratings," J. Opt. Soc. Am. **72,** 187–190 (1982).
8. H. A. Macleod, *Thin-Film Optical Filters,* 3rd ed. (Institute of Physics Publishing, 2001).
9. H. Kogelnik, "Coupled wave theory for thick hologram gratings," Bell Syst. Tech. J. **48,** 2909–2947 (1969).
10. O. M. Efimov, L. B. Glebov, and V. I. Smirnov, "Diffractive optical elements in photosensitive inorganic glasses," in *Inorganic Optical Materials III*, A. J. Marker III and M. J. Davis, eds., Proc. SPIE **4452,** 39–47 (2001).